Potent antitumour activity of (–)epigallocatechin gallate: indications from *in vitro*, *in vivo* and *in silico* studies

Samarendra Narayanan[1],*, **Balaji Ramchandran[2]**, **Satheesh Rajendiran[2]**, **Sarbani Chandra[2]**, **Atul Tiwari[2]**, **Ravisankar Rajarethinam[3]** and **Ramesh Kureeckal Vasudev[1]**

[1]Department of Biotechnology, Center for Post-graduate Studies, Jain University, Bengaluru 560 011, India
[2]Department of Biology, Syngene International Limited, Jigani Link Road, Bengaluru 560 011, India
[3]Institute of Molecular and Cell Biology, Biopolis, Singapore

Antitumour efficacy of (–)epigallocatechin-3-gallate (EGCG) was evaluated *in vitro* against the cancer cell lines BxPC-3 (pancreatic cancer), A549 (lung cancer), SH-SY5Y (neuroblastoma), MDA-MB-231 and MCF-7 (breast cancer); *in vivo* in nude mice by tumour growth inhibition of pancreatic cancers (BxPC-3, MIAPaCa-2), breast cancer (MDA-MB-231), and *in silico* by docking studies. EGCG significantly inhibited these cancer cell lines *in vitro* and showed significant tumour reduction *in vivo*. EGCG docked on to the Her-2 receptor (1N8Y) and the tubulin dimer receptor at a site other than the existing docetaxel ligand. Overall our results suggest that EGCG has potent antineoplastic activity.

Keywords: Antitumour efficacy, breast cancer, docking, epigallocatechin gallate, lung cancer.

CANCER is the deadliest of all diseases known to mankind. Despite significant advances in cancer therapy in recent years, the mean survival time, even after aggressive therapy, remains low. According to the Global Cancer Report (GLOBOCAN), in 2012 there were 14.1 million new cases worldwide[1]. Presently various anticancer drugs are administered in combination with radiation therapy. Not only is the treatment for cancer expensive, but it also has severe side effects.

Pancreatic cancers, a group of extremely aggressive human cancers, have been reported to cause 330,391 deaths worldwide annually[1], while the overall 5-year survival rate remains less than 5% (ref. 2). Conventional treatments have little impact on the progression of pancreatic cancers[3]. Breast cancer is the leading type of cancer in women, accounting for 25% of all cases, and causing 522,000 deaths worldwide annually[1]. Treatment is often accompanied by severe side effects. Prostate cancer, one of the most aggressive cancers in men with a 5-year survival rate of less than 5%, is resistant to conventional chemotherapeutic agents. It has high morbidity and an estimated annual mortality of more than 307,481 deaths[1]. Small-cell lung cancer is a highly malignant cancer that most commonly arises within the lung and occasionally in the cervix, prostrate and gastrointestinal tract. Relapse is common with a median survival time of only 12–18 months[1].

Epigallocatechin gallate (EGCG), a green tea polyphenol is known to inhibit cell proliferation and induce apoptosis in a variety of human neoplasms[4–6].

Recently, some compounds from natural products targetting tubulin have been discovered such as epothilone, paclitaxel, colchicines and vindesine[7–9]. Previous studies on EGCG have attempted to examine the antitumour activity employing *in vitro* or *in vivo* methods[6,10].

We report here, the anticancer activity of EGCG in addition to the *in vitro*, *in vivo* and immunohistochemical (IHC) studies conducted, and the *in silico* aspects of inhibition of HER 2 tyrosin kinase receptor and tubulin dimer receptor 1 TUB (already containing docetaxel ligand) with the help of docking studies. Besides studying the docking of EGCG with Her2 receptor (1N8Y), we also examined the *in silico* aspect of microtubule polymerization for the inhibition of tumour cell growth. In the mitotic phase of the cell cycle, microtubules maintain dynamic equilibrium with tubulin dimers by assembling the tubulin into microtubules or, conversely, disassembling microtubules to tubulin[7]. Disruption of the dynamic equilibrium can induce cell-cycle arrest and ultimately lead to apoptosis.

Materials and methods

EGCG (Carbosynth, Berkshire, UK) was dissolved in sterile 1 mM phosphate buffered saline (PBS) to obtain a clear solution.

*For correspondence. (e-mail: sam19narayan@yahoo.co.in)

Cell culture

Cancer cell lines procured from the American Type Culture Collection (ATCC) (Manassas, VA, USA) included BxPC-3, MIAPaCa-2 (human pancreatic adenocarcinoma); A549 (human lung carcinoma); Caco-2 (human colorectal adenocarcinoma); MDA-MB-231, MCF-7 (human breast adenocarcinoma) and SH-SY5Y (human neuroblastoma). These cell lines were cultured in DMEM (GIBCO, Life Technologies, NY, USA), supplemented with 10% foetal bovine serum (FBS) and penicillin–streptomycin. The cells were subjected to media change every 2–3 days, subcultured after 80% confluence was attained and then dislodged using 0.25% trypsin–EDTA solution.

Cell proliferation/cytotoxicity assay

Here, 100 µl of cells was seeded at a density of 5000 cells/well in a black 96-well clear bottom plate (Sigma Aldrich, MO, USA) and allowed to adhere in a humidified incubator at 37°C and 5% CO_2 for 2–3 h before addition of the EGCG. The initial concentration of IC_{50} was finalized based on results from a three-concentration screening test carried out earlier. EGCG was diluted as required and 100 µl of the solution was added to the cells. Respective controls for the vehicle and 100% cytotoxicity were also added. The plates were incubated in a humidified incubator at 37°C and 5% CO_2 for 48 h. Post-incubation, the medium was discarded from the plates by gentle flicking, and replaced with 100 µl of 1× Cell Titer-Blue® (Promega, WI, USA) solution. The plates were further incubated at 37°C for 1 h and subsequently read on a molecular reader (Molecular Devices Flex Station III, Molecular Devices, CA, USA) using excitation and emission wavelengths of 560 and 590 nm respectively. Viability of the cells (%) was determined by dividing the blank-corrected average relative fluorescence units (RFUs) for each concentration over the blank-corrected average RFU of the vehicle control. IC_{50} was determined using GraphPad Prism Software (GraphPad SoftwareInc, CA, USA). Three replicates were performed for each dilution and the average was taken for comparison.

Human tumour xenografts

Athymic female nude mice (Hsd: Athymic Nude-Foxn1[nu]), 5–6 weeks old, and weighing 20–22 g were obtained from Harlan, The Netherlands. Animals were cared for in compliance with the regulations of the Committee for the Purpose of Control and Supervision of Experiments on Animals (CPCSEA), Government of India and the Association for Assessment and Accreditation of Laboratory Animal Care (AAALAC), GoI. The protocol for carrying out animal experimentation was reviewed and approved by the Institutional Animal Ethics Committee of the facility.

Three xenograft experiments were conducted as follows: In the first experiment, BxPC-3 xenograft-bearing mice ($n = 5$) were treated with EGCG at a dosage of 80 mg/kg, i.p. on days 0, 3, 6, 9, 12 and 15 (Q3D × six doses). Mice ($n = 5$) bearing tumour but left untreated were used as controls. In the second xenograft experiment, mice ($n = 5$) bearing the MIAPaCa-2 tumours were administered EGCG at a dose of 80 mg/kg, i.p. on days 0, 3, 6 and 9 (Q3D × four doses). In the third xenograft experiment with mice bearing MDA-MB-231 tumours, EGCG was administered at a dose of 90 mg/kg, i.p. on day 0, 3, 6 and 9 (Q3D × four doses). Animals were maintained in a controlled environment in individually ventilated cages.

All procedures were performed in a bio-safe cabinet following sterile techniques. BxPC-3, MIAPaCa-2 and MDAMB-231 cell lines with 70–80% confluent and >90% viability were chosen for the study. Then $5 × 10^6$ cells were suspended in 200 µl of cold PBS or serum-free media containing 50% matrigel kept in an ice-bath. The above-mentioned cell lines were propagated in the animals by injecting them subcutaneously in the flanks or at the back of the animals. The implanted area was monitored for growth of tumour. Once the tumour attained palpable and required volume, the animals were randomized based on tumour volume and dosing was initiated. The mice were weighed and tumour volume was determined by measuring the dimensions of the tumour in two mutually perpendicular directions with vernier calipers on the day of randomization (day 0) and once every three days thereafter[11]. Cage-side observations were recorded and change in body weight (%) of individual mice was calculated. Animals were observed individually for visible clinical signs of morbidity and mortality. The animals were euthanized after final observation and the tissues were collected for histopathology and immune-histochemical (IHC) staining.

Antitumour activity

Mean volume of the tumour on EGCG-treated mice (T) on any observation day was compared to mean tumour volume of control mice (C). Antitumour activity on a particular day was taken as a ratio of T to C expressed as percentage, i.e. $(T/C) × 100$.

Tumour growth inhibition

On each observation day, tumour growth inhibition (TGI) was calculated as $(1 - T/C) × 100$.

Immunohistochemistry

BxPC-3 tumour tissue from euthanized control as well as EGCG-treated animals was subjected to IHC study using

antibody generated against Ki-67, a mitotic (proliferative) marker, following a slightly modified protocol based on Lee *et al.*[10]. Tumour tissue was fixed in 10% buffered neutral formalin for one day, post-fixed with 70% alcohol, then processed in an automatic tissue processor (Leica Biosystem), progressively dehydrated using ascending grades of isopropyl alcohol and finally cleared with xylene. Dehydrated tissue was embedded in paraffin block, sectioned at 3–5 μm size, taken onto a poly-L-lysine slide and IHC staining was performed. After deparaffinization, heat-induced epitope antigen retrieval was carried out by treating the slides with 10 mM citrate buffer, pH 6.0, for 10 min at 121°C in a decloaking chamber (DC2002 INTL, Biocare Medicals, USA). Endogenous peroxidase was quenched using 3% H_2O_2 and blocked at room temperature for 15 min, followed by protein block (background punisher) carried out for 15 min at room temperature. The tissue sections were incubated with primary antibody, anti-human Ki-67 rabbit monoclonal antibody (CRM 325, ABC Biocare Medicals, USA) for 1 h in a humidified chamber at room temperature. Negative controls were run in parallel and treated with PBS instead of a specific antibody solution under identical conditions. MACH 4 detection kit (M4U534G, H, L MM) was used for the detection of Ki-positive reaction in the cells. MACH 4 probe was added and incubated for 10 min. Following incubation, MACH 4 HRP polymer was added and the colour of the sections was visualized by treatment with diaminobenzidine (DAB). The sections were counterstained with Mayer's hematoxylin followed by dehydration, clearing and mounting. The evaluation of tumour cells expressing Ki-67 was performed at 40× magnification by an independent observer blinded to the protocol. For each slide, 15 representative photomicrographs at high magnification were taken, and positive-stained cancer cells and total number of cells were counted using Leica Analysis Suite (LAS) image processing program (Leica Microsystem, Germany). Ki-67 proliferation index was calculated as the percentage of positively stained cells to total cells. The tumour tissue was also analysed for the presence of necrosis with Leica analysis software.

In silico studies

Two-dimensional structure of EGCG was drawn using GAUSSVIEW package (Gaussian Inc, CT, USA) followed by optimization of the geometry using GAUSSIAN package as detailed elsewhere[12]. Hatree–Fock theory with '6-31++g (d, p)' as the basis set was used for optimizing the structures. Standard orientation of EGCG after convergence to its global energy minima was visualized using ARGUS package (Argus Lab, WA, USA) before the docking exercise[13], and was saved in PDB format. Geometrically optimized EGCG was later docked using Hex ver. 6.0 software[14] onto the crystal structure of epidermal growth factor receptor from *Rattus norvegicus* (PDB ID: 1N8Y)[15]. The optimized EGCG structure was also docked onto the crystal structure of $\alpha\beta$ tubulin heterodimer, a structural subunit of microtubules from *Sus scrofa* complexed with docetaxel (PDB ID: 1TUB)[16]. Docking energy in each case was calculated based on the shape and electrostatics using default grid spacing of 6.0 Å.

Statistical analysis

All comparisons of mean antitumour activity and mean TGI were done using Student's *t*-test and GraphPad Prism v5. *P* value less than 0.05 indicates statistically significant differences between groups (95% CI).

Results

EGCG inhibits growth of cancer cells

Figure 1 depicts the growth inhibition curves for various tumour cell lines by EGCG. Table 1 shows the 50% inhibition concentration (IC_{50}) values for each of these cell lines. The dose–response curves indicate that EGCG is cytotoxic to all the cancer cell lines examined and inhibits the growth of these cells in a dose-dependent manner.

EGCG inhibits tumour growth in mouse models

Based on the observed inhibition of the growth of these cancer cell lines *in vitro*, anticancer activity of EGCG was evaluated in xenograft-bearing nude mice models induced by subcutaneous injection of the pancreatic cancer cell lines, BxPC-3 and MIAPaCa-2, and breast cancer cell line MDA-MB-231.

BxPC-3: Figure 2 *a* shows the mean body weight of control and EGCG-treated mice harbouring BxPC-3 tumour, while Figure 2 *b* depicts tumour volume determined on various observation days. There was no loss of body weight in vehicle control and EGCG-treated mice during the experimental period. All animals were active and healthy. EGCG therapy was relatively well tolerated at the tested dose level with no mortality. Moreover, there were no visible signs of abnormal behaviour or any adverse clinical symptoms during treatment. EGCG showed a strong antitumour activity *in vivo* when injected in nude mice at a dose of 80 mg/kg. Treatment with EGCG resulted in an optimal ratio (*T/C*) of mean tumour volume of treated mice (*T*) to that of control mice (*C*), of 19% on day 15. TGI for the EGCG group at the tested dose level was found to be 80.9% (day 15, *P* < 0.001).

MIAPaCa-2: As shown in Figure 3 *a*, there was no significant loss of body weight in vehicle control and
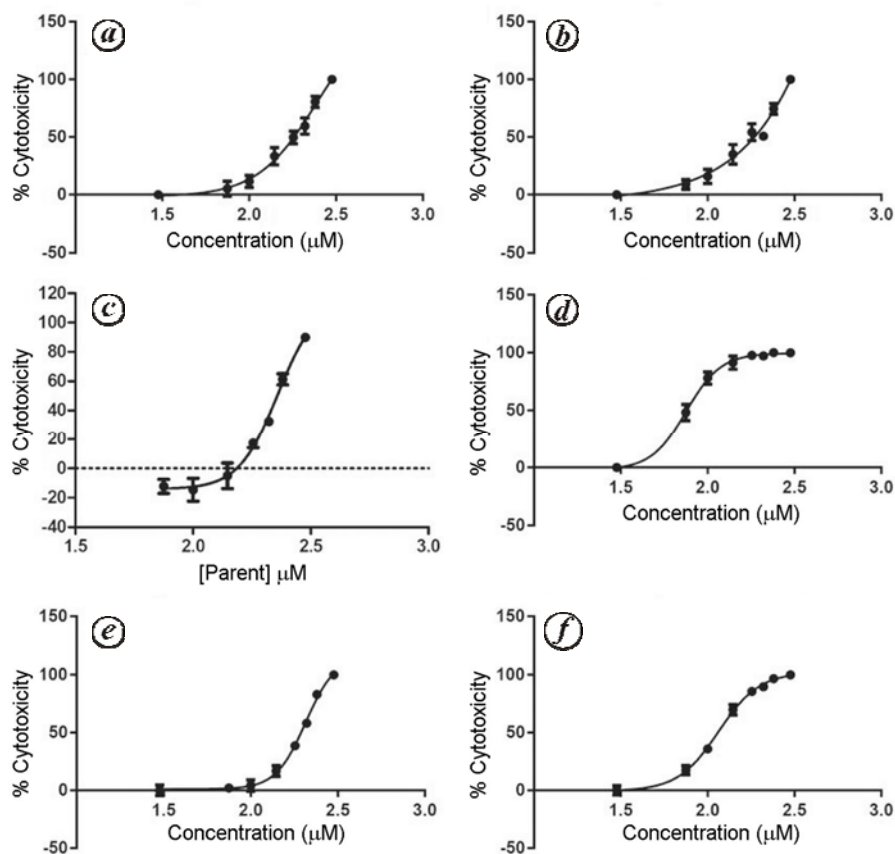
Figure 1. Dose-response curves for the inhibition of various tumour cell lines by (–)epigallocatechin-3-gallate (EGCG): *a*, BxPC-3; *b*, A549; *c*, Caco-2; *d*, SH-SY5Y; *e*, MDA-MB-231; *f*, MCF-7. Values shown on *x*-axis are log[EGCG] (μM).

Table 1. IC50 concentrations of (–)epigallocatechin-3-gallate (EGCG) for various cell lines

Cell line	IC50 (μM)
BxPC-3	245.9
A549	191.2
Caco-2	228.5
SH-SY5Y	75.1
MDA-MB-231	206.8
MCF7	115.6

EGCG-treated group during the experimental period. EGCG therapy was relatively well tolerated at the tested dose level with no mortality. Moreover, there were no visible signs of abnormal behaviour or any adverse clinical symptoms during treatment. Figure 3 *b* shows the tumour growth curve for control as well as EGCG-treated group. EGCG demonstrated significant ($P < 0.001$) antitumour activity against MIAPaCa-2 xenograft tumour model. Treatment with EGCG was continued only up to day 9, but post-treatment observation was continued up to day 24. The results show an optimal T/C of 44.5% on the day 24. TGI for EGCG group at the tested dosage was found to be 55.45% (day 24, $P < 0.001$).

MDA-MB-231: EGCG was relatively well tolerated at the tested dose level (90 mg/kg) with no mortality. There was no significant loss in body weight in vehicle control as well as EGCG-treated group during the experimental period (Figure 4 *a*). Based on cage side observations, there were no visible signs of abnormal behaviour or clinical symptoms in the EGCG-treated group. In the dosage regime studied, EGCG treatment demonstrated significant ($P < 0.001$) antitumour activity (Figure 4 *b*) against MDA-MB-231 xenograft tumour model, with an optimal T/C of 45.4% on day 45. TGI for the EGCG group at the tested dose level was found to be 54.59% (day 45, $P < 0.001$).

Histopathology and immunohistochemistry

Histopathological examination of the tumour tissue (BxPC-3) obtained from all the animals showed encapsulation under the subcutaneous tissue (Figure 5 *a* and *b*). Pleomorphic malignant epithelial cells were arranged in cord or acinar pattern. These tumour cells were surrounded by abundant fibrous stroma. Individual tumour cells contained vacuolation in the cytoplasm. The tumour

also showed the presence of keratinized epithelial cells forming the pearls. We observed that the area of necrosis was more predominant in EGCG-treated animals than the control group. The average area of necrosis was 2.86 ± 0.94 mm^2 in the control animals, while it increased to 6.64 ± 2.14 mm^2 in EGCG-treated animals. Figure 5 c shows the mean area of necrosis as measured by image analysis.

Figure 6 a and b shows the IHC staining of BxPC-3 tumour tissues from control as well as EGCG-treated animals. The expression of Ki-67 positive cells was significantly lower ($P < 0.05$) in EGCG-treated animals (777.97 ± 84.90/mm^2) than control animals (1388.32 ± 117.04/mm^2; Figure 6 c). EGCG significantly inhibited tumour cell growth in the xenograft animal model (56%). This effect was further demonstrated by the finding that the proliferation index significantly reduced ($P < 0.05$) to 22% after EGCG treatment (Figure 6 d) in comparison to saline control (46%).

In silico docking studies

Figure 7 shows the energy-minimized structure of EGCG. Table 2 lists the results of minimization using Gaussian.

Convergence was achieved for all the parameters after 11 cycles.

The geometrically optimized ligand EGCG was docked successfully onto the tyrosine receptor kinase (Herceptin, PDBID : 1N8Y) using the HEX docking program (Figure 8 a). The docking energy was -302.09 kcal mol^{-1}. The neighbouring residues for EGCG, as depicted in Figure 8 b, are:

asn^{298}, gln^{299}, glu^{300,383,384}, val^{301}, thr^{302}, ala^{318}, arg^{319,408,411}, val^{320}, cys^{321}, tyr^{322}, cys^{321,346}, lys^{347,348}, ile^{349,385,409}, phe^{350} and leu^{382}.

EGCG was also docked onto the experimentally determined structure of tubulin $\alpha\beta$ dimer complexed with TXL from *S. scrofa* (PDB ID: 1TUB) (Figure 9 a). Geometrically optimized EGCG was able to dock at a site different from that of docetaxel. The docking energy was -302.6 kcal mol^{-1}. EGCG interacts with the neighbouring residues in both A and B chains (Figure 9 b), while docetaxel interacts with residues from the B chain only (Figure 9 c). The neighbouring residues observed in the
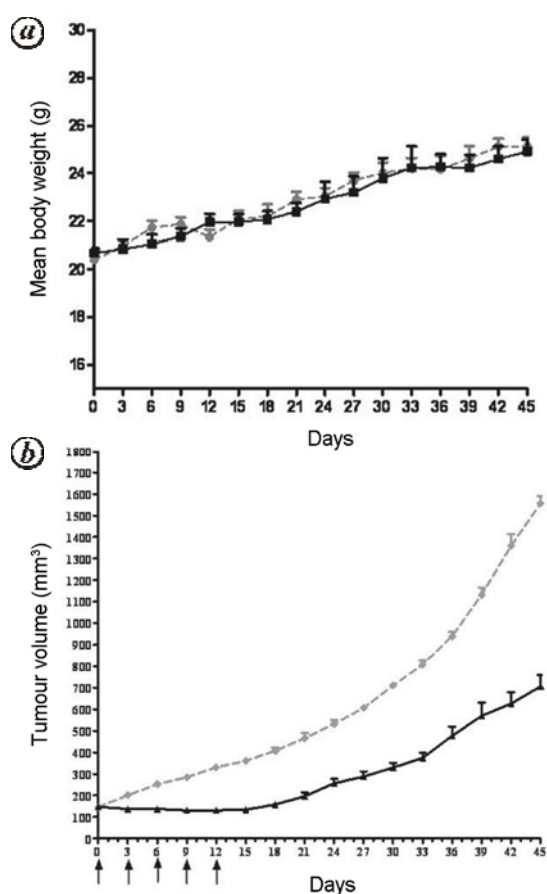
Figure 2. Effect of EGCG on BxPC-3 tumour induced in nude mice at the tested dose of 80 mg/kg (day 15, $P < 0.001$): (**a**) mean body weight and (**b**) tumour volume of EGCG-treated and control animals.
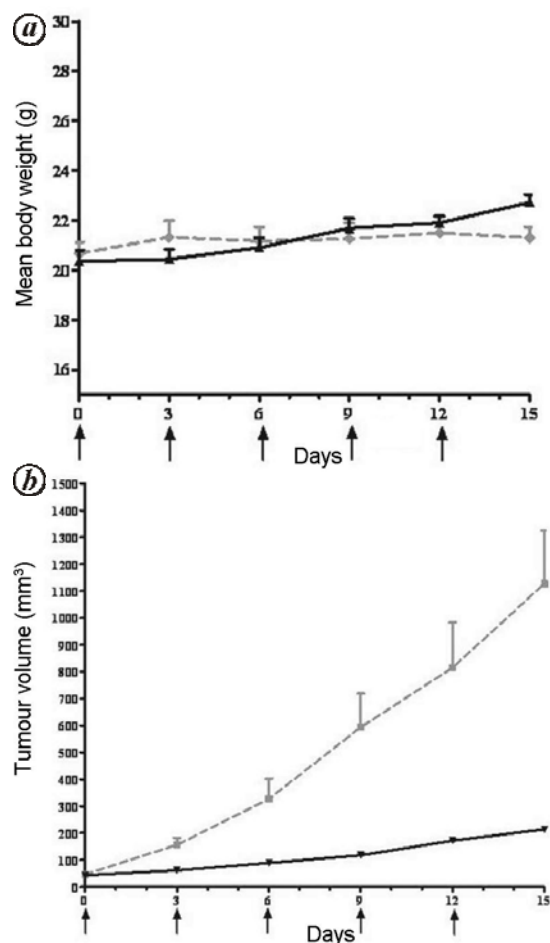
Figure 3. Effect of EGCG on MIAPaCa-2 tumour induced in nude mice at the tested dose of 80 mg/kg (day 24, $P < 0.001$): (**a**) mean body weight and (**b**) tumour volume of EGCG-treated and control animals.
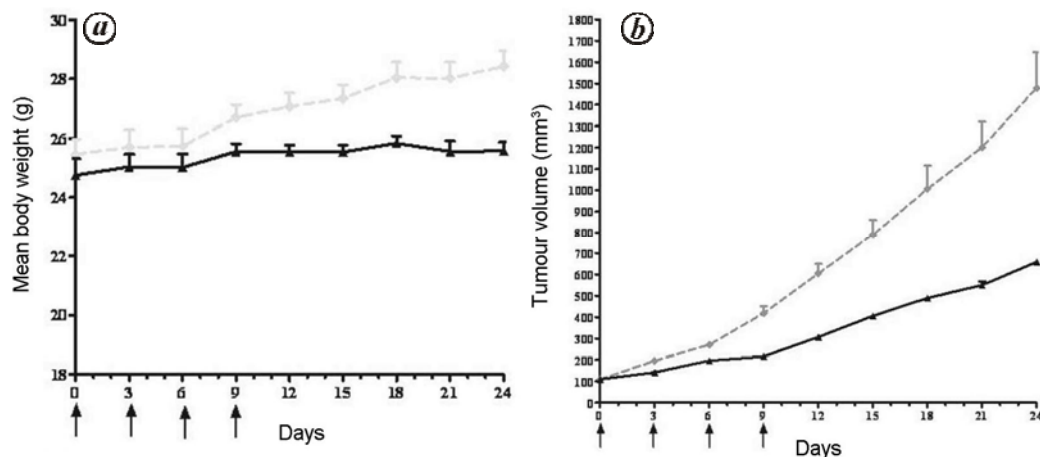
Figure 4. Effect of EGCG on MDA-MB-231 tumour induced in nude mice at the tested dose of 90 mg/kg (day 45, $P < 0.001$): (*a*) mean body weight and (*b*) tumour volume of EGCG-treated and control animals.
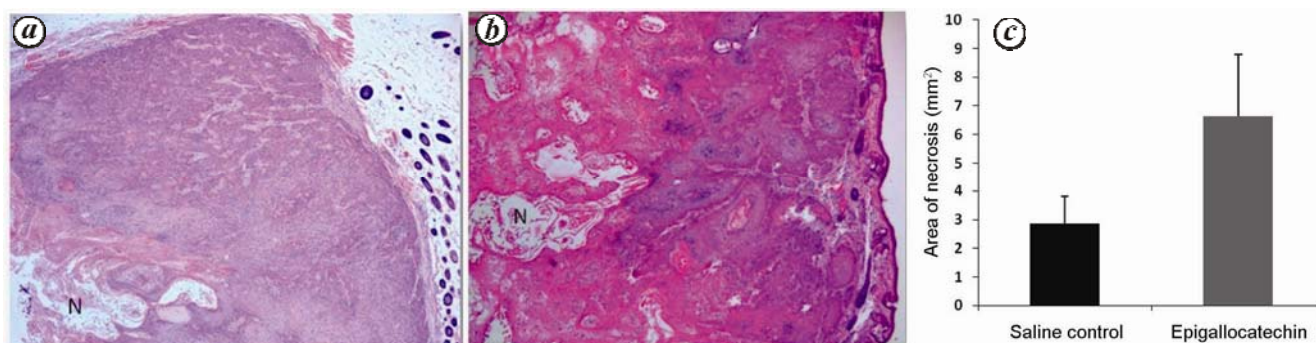
Figure 5. Effect of EGCG on the growth of BxPC-3-induced pancreatic xenograft in nude mice. Tumour cells showing area of necrosis tumour cells (asterisk) in (*a*) EGCG-treated and (*b*) saline control animals (H&E stain, x4). (*c*) Area of necrosis (mean ± SE) in saline control and EGCG-treated mice as measured by image analysis.

Table 2. Energy minimization parameters of EGCG

Parameter	Value	Threshold	Convergence
Maximum force	0.000025	0.000450	Yes
RMS force	0.000005	0.000300	Yes
Maximum displacement	0.001478	0.001800	Yes
RMS displacement	0.000334	0.001200	Yes
Predicted change in energy		−1.895627E-08	
Optimization completed			
Stationary point found			

vicinity (within 6 Å) of EGCG (in the docked structure) are as follows

A chain: $gly^{95,106,410}$, lys^{96}, $glu^{97,113,411}$, ala^{99}, arg^{105}, tyr^{108}, thr^{109}, ile^{110}.

B chain: met^1, arg^2, glu^3, $asp^{130,163}$, lys^{131}, leu^{132}, gln^{133}, gly^{134}, glu^{160}, tyr^{161}, pro^{162}, $arg^{164,253}$, ile^{165}.

The neighbouring residues in the vicinity of TXL (Figure 9 *c*) belong to the B chain only and are

B chain: $lys^{19,372}$, glu^{22}, val^{23}, $asp^{26,226}$, $phe^{83,272}$, $leu^{217,219,227,230,275,371}$, $thr^{223,276}$, $gly^{225,237,370}$, his^{229}, $ser^{232,236,277}$, ala^{233}, $pro^{274,359,360}$, $arg^{278,320,369}$, gln^{281}, asn^{228}.

In silico studies confirm the docking of EGCG with 1N8Y as well as 1TUB receptors to a similar extent, as indicated by the calculated docking energies.

Discussion

In this study EGCG shows significant antitumour activity as seen from the results of *in vitro*, *in vivo*, IHC and *in silico* docking studies. The observation of significant TGI, 80.9% against BxPC-3, 55.5% against MIAPaCa-2 and 55.6% against MDA-MB-231 tumours strongly indicates that EGCG could be considered as a valuable adjunct to the battery of frontline anticancer compounds. The histological observations of significant destruction of BxPC-3 tumour cells, are evidenced by increased necrosis in EGCG-treated animals compared to untreated
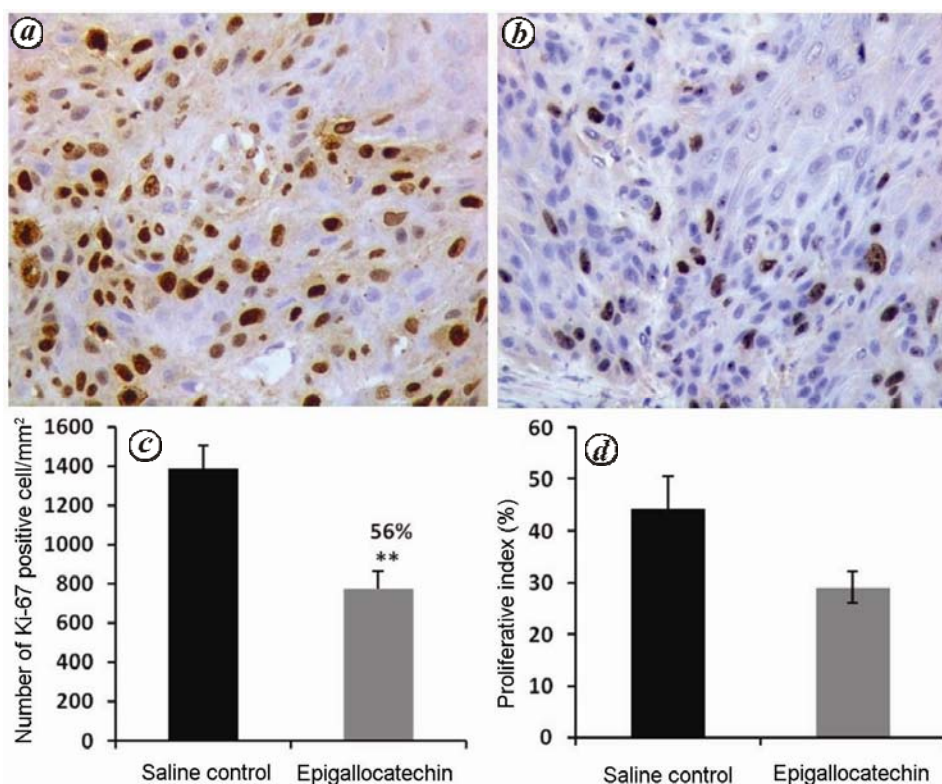
Figure 6. Representative photomicrographs of tumour cells showing the effect of EGCG on the proliferation of Ki-67 marker, in BxPC-3 induced mouse xenograft. (*a*) Vehicle control and (*b*) EGCG-treated mice (immunoperoxidase stain, x40). *c*, Expression of Ki-67 is significantly reduced (56%) in EGCG-treated mice ($P < 0.05$). *d*, Ki-67 proliferation index is significantly reduced by EGCG ($P < 0.05$).
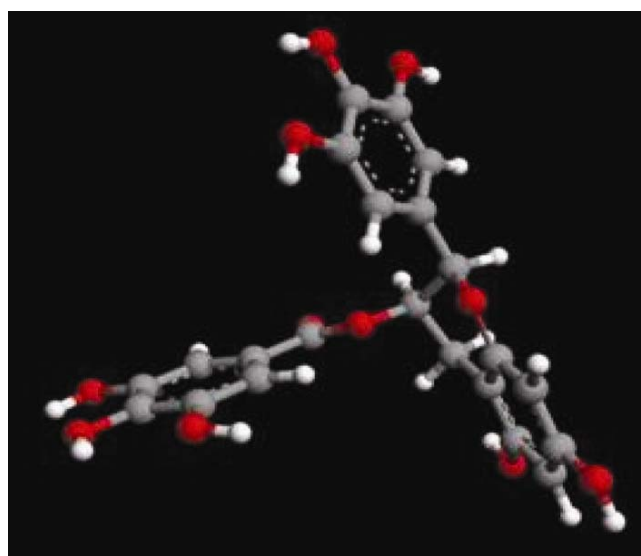
Figure 7. Geometrically optimized EGCG, [E (RHF) = –1667.05 U after 11 cycles].

control. The results of immunohistochemistry show significantly reduced expression of the proliferation marker Ki-67 in tumours of nude mice treated with EGCG, compared to untreated controls. Further, results of the docking studies corroborate the *in vitro*, *in vivo* and IHC findings as demonstrated by docking of EGCG to the Her2 receptor (1N8Y) with a good docking energy and in the case of the microtubule receptor, 1TUB, at a site away from that of docetaxel. Further, EGCG is also observed to interact with neighbouring residues in both A
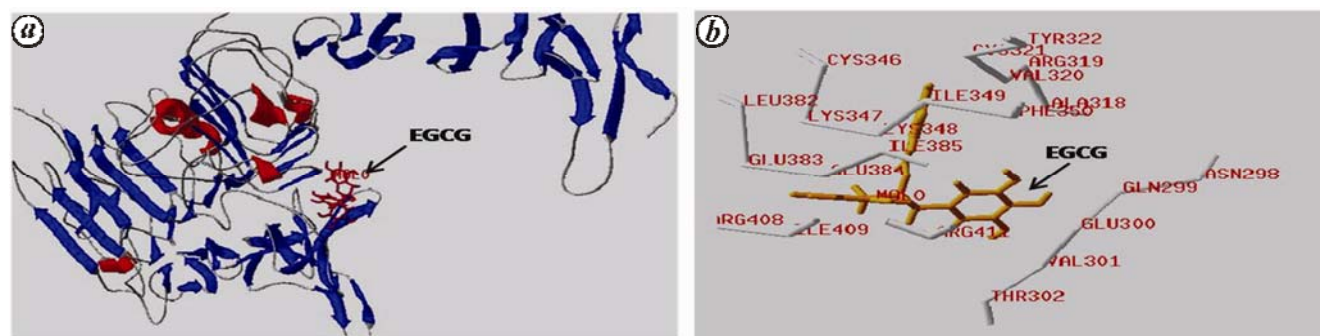
Figure 8. *a*, Docking of geometrically optimized EGCG with 1N8Y receptor. MOL0 represents EGCG. *b*, Neighbouring residues of EGCG (in gold yellow). Images generated using Deep View package[18].
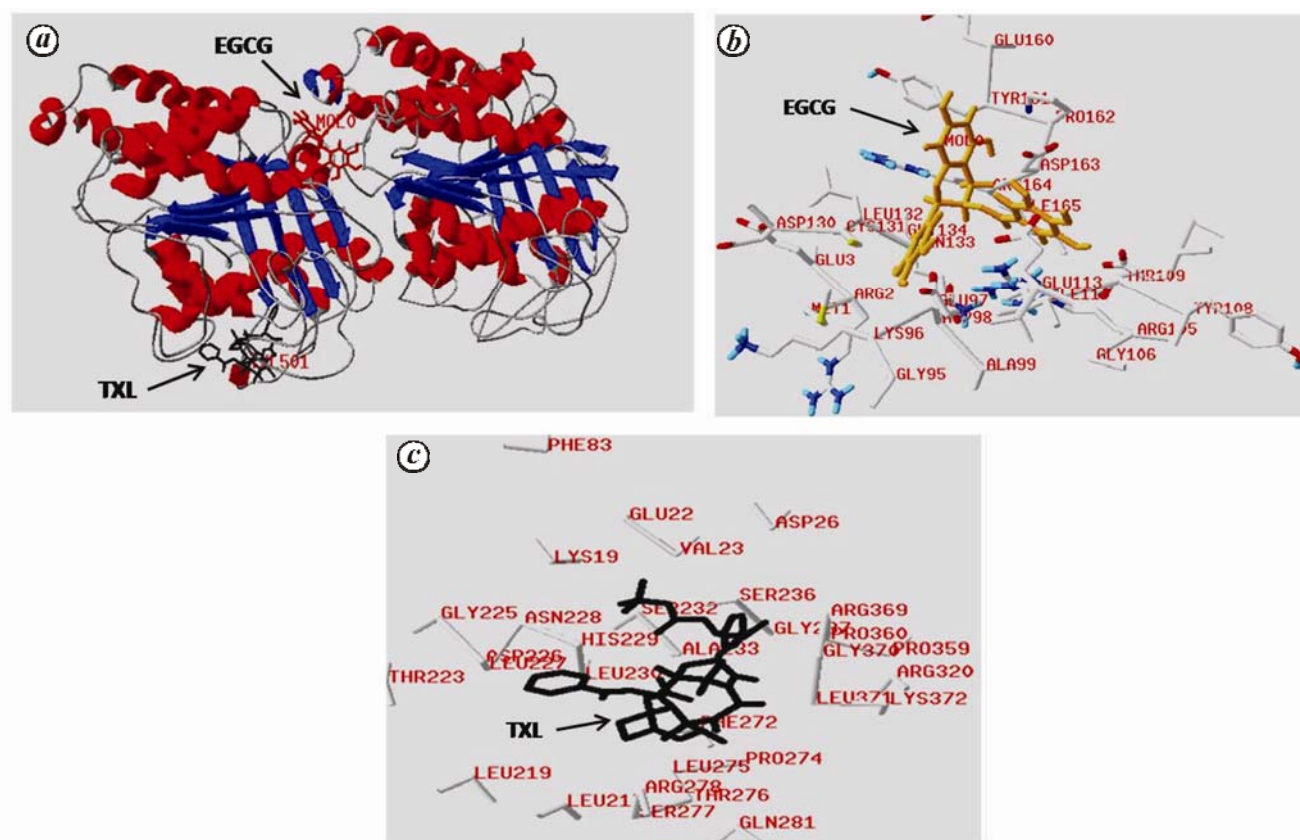
Figure 9. *a*, Docking of geometrically optimized EGCG onto 1TUB tubulin $\alpha\beta$ dimer complexed with docetaxel (TXL). MOL0 represents EGCG, while 501 represents TXL. *b*, *c*, Neighbouring residues in the vicinity of (*b*) EGCG and (*c*) TXL. Images generated using DeepView package[18].

and B chains while docetaxel is seen interacting only with residues from the B chain, which may indicate a potentially complementary action in binding to the microtubule network.

EGCG, the major component of green tea, is known to be capable of inhibiting the growth of a variety of human cancer cells via the induction of apoptosis[17]. The finding of marked cell destruction is well supported by the observation of reduced number of viable cells on treatment with epigallocatechin, in human lung cancer H1299 cells

in culture and in xenograft tumour reported by Li *et al.*[18]. In the present study, morphometric evaluation of cell death clearly indicates the effect of EGCG on viable cells. Studies have also shown that polyphenols from green tea possess antitumour and anti-metastatic properties in animal xenograft and allograft models, suggesting a possible therapeutic potential[19]. Vu *et al.*[2] have also supported possible use of EGCG in reducing metastasis of pancreatic cancer, although EGCG alone has limited effect on cell growth inhibition[5].

Treatment for neuroblastoma, is usually through multi-therapy with radiation, surgery and chemotherapy. Canete et al.[20] reported poor response to treatment and the urgent need for new approaches to therapy for this type of cancer. In the present study, EGCG has shown strong inhibition of the neuroblastoma cell line, SHY5Y, in the *in vitro* model. It has also shown a dose-dependent inhibition of A549, a highly malignant, small-cell lung cancer cell line, and deserves further evaluation in combination therapy.

Summary

EGCG has been evaluated earlier by *in vitro* and *in vivo* studies. Here, in addition to the above, we also conducted IHC and docking studies. Taken together, the results indicate that EGCG demonstrates significant antitumour activity, which may open new vistas in combination anti-cancer therapy.

1. Fact sheets by cancer, International Agency for Research on Cancer, France; http://globocan.iarc.fr/Pages/fact_sheets_cancer.aspx; (updated January 2015; cited 14 February 2015).

2. Vu, H. A. *et al.*, Green tea epigallocatechin gallate exhibits anti-cancer effect in human pancreatic carcinoma cells via the inhibition of both focal adhesion kinase and insulin-like growth factor-I receptor. *J. Biomed. Biotechnol.*, 2010, 290516.

3. Tang, S. N., Fu, J., Shankar, S. and Srivastava, R. K., EGCG enhances the therapeutic potential of gemcitabine and CP690550 by inhibiting STAT3 signaling pathway in human pancreatic cancer. *PLoS ONE*, 2012, **7**, 31067.

4. Asano, Y., Okamura, S., Ogo, T., Eto, T., Otsuka, T. and Niho, Y., Effect of (–)-epigallocatechin gallate on leukemic blast cells from patients with acute myeloblastic leukemia. *Life Sci.*, 1997, **60**, 135–142.

5. Hibasami, H. *et al.*, Induction of apoptosis in human stomach cancer cells by green tea catechins. *Oncol. Rep.*, 1998, **5**, 527–529.

6. Paschka, A. G., Butler, R. and Young, C. Y., Induction of apoptosis in prostate cancer cell lines by the green tea component, (–)-epigallocatechin-3-gallate. *Cancer Lett.*, 1998, **130**, 1–7.

7. Hyams, J. S. and Stebbings, H., The mechanism of microtubule associated cytoplasmic transport. Isolation and preliminary characterisation of a microtubule transport system. *Cell Tissue Res.*, 1979, **196**, 103–116.

8. Valiron, O., Caudron, N. and Job, D., Microtubule dynamics. *Cell Mol. Life Sci.*, 2001, **58**, 2069–2084.

9. Sengupta, S. and Thomas, S. A., Drug target interaction of tubulin-binding drugs in cancer therapy. *Expert Rev. Anticancer*, 2006, **6**, 1433–1447.

10. Lee, S. C. *et al.*, Effect of a prodrug of the green tea polyphenol (–)-epigallocatechin-3-gallate on the growth of androgen-independent prostate cancer *in vivo*. *Nutr. Cancer*, 2008, **60**, 483–491.

11. Teicher, B. A. (ed.), *Tumor Models in Cancer Research*, Humana Press, Totowa, NJ, 2011; http://link.springer.com/10.1007/978-1-60761-968-0 (cited 14 February 2015).

12. Pople, J. A., Head-Gordon, M., Fox, D. J., Raghavachari, K., Curtiss, L. A., Gaussian-1 theory: a general procedure for prediction of molecular energies. *J. Chem. Phys.*, 1989, **90**, 5622–5629.

13. Arguslab; http://www.arguslab.com/arguslab.com/ArgusLab.html (cited 14 February 2014).

14. Ritchie, D. W. and Venkatraman, V., Ultra-fast FFT protein docking on graphics processors. *Bioinformatics*, 2010, **26**, 2398–2405.

15. Cho, H. S. *et al.*, Structure of the extracellular region of HER2 alone and in complex with the Herceptin Fab. *Nature*, 2003, **421**, 756–760.

16. Nogales, E., Wolf, S. G. and Downing, K. H., Structure of the alpha beta tubulin dimer by electron crystallography. *Nature*, 1998, **391**, 199–203.

17. Chan, M. M., Soprano, K. J., Weinstein, K. and Fong, D., Epigallocatechin-3-gallate delivers hydrogen peroxide to induce death of ovarian cancer cells and enhances their cisplatin susceptibility. *J. Cell. Physiol.*, 2006, **207**, 389–396.

18. Li, G. X. *et al.*, Pro-oxidative activities and dose-response relationship of (–)-epigallocatechin-3-gallate in the inhibition of lung cancer cell growth: a comparative study *in vivo* and *in vitro*. *Carcinogenesis*, 2010, **31**, 902–910.

19. Baliga, M. S., Meleth, S. and Katiyar, S. K., Growth inhibitory and antimetastatic effect of green tea polyphenols on metastasis-specific mouse mammary carcinoma 4T1 cells *in vitro* and *in vivo* systems. *Clin. Cancer Res.*, 2005, **11**, 1918–1927.

20. Canete, A. *et al.*, Poor survival for infants with MYCN amplified metastatic neuroblastoma despite intensified treatment: The International Society of Pediatric Oncology European Neuroblastoma Experience. *J. Clin. Oncol.*, 2009, **27**, 1014–1019.